ADVANCES IN ATMOSPHERIC SCIENCES, VOL. 22, NO. 6, 2005, 865–876

Numerical Simulation of the Impact of Vegetation Index on the Interannual Variation of Summer Precipitation in the Yellow River Basin

LI Weiping*[1] (李伟平) and XUE Yongkang[2] (薛永康)

[1] *Laboratory for Climate Studies, National Climate Center, China Meteorological Administration, Beijing* 100081

[2] *Department of Geography and Department of Atmospheric Sciences, University of California at Los Angeles, California, USA*

(Received 1 February 2005; revised 24 June 2005)

ABSTRACT

Two sets of numerical experiments using the coupled National Center for Environmental Prediction General Circulation Model (NCEP/GCM T42L18) and the Simplified Simple Biosphere land surface scheme (SSiB) were carried out to investigate the climate impacts of fractional vegetation cover (FVC) and leaf area index (LAI) on East Asia summer precipitation, especially in the Yellow River Basin (YRB). One set employed prescribed FVC and LAI which have no interannual variations based on the climatology of vegetation distribution; the other with FVC and LAI derived from satellite observations of the International Satellite Land Surface Climate Project (ISLSCP) for 1987 and 1988. The simulations of the two experiments were compared to study the influence of FVC, LAI on summer precipitation interannual variation in the YRB. Compared with observations and the NCEP reanalysis data, the experiment that included both the effects of satellite-derived vegetation indexes and sea surface temperature (SST) produced better seasonal and interannual precipitation variations than the experiment with SST but no interannual variations in FVC and LAI, indicating that better representations of the vegetation index and its interannual variation may be important for climate prediction. The difference between 1987 and 1988 indicated that with the increase of FVC and LAI, especially around the YRB, surface albedo decreased, net surface radiation increased, and consequently local evaporation and precipitation intensified. Further more, surface sensible heat flux, surface temperature and its diurnal variation decreased around the YRB in response to more vegetation. The decrease of surface-emitting longwave radiation due to the cooler surface outweighed the decrease of surface solar radiation income with more cloud coverage, thus maintaining the positive anomaly of net surface radiation. Further study indicated that moisture flux variations associated with changes in the general circulation also contributed to the precipitation interannual variation.

Key words: numerical simulation, vegetation index, interannual variation, summer precipitation, Yellow River basin

1. Introduction

Most parts of north China experience the rainy season from June to August (Chen et al., 1991), coinciding with the East Asian summer monsoon, the formation and intensity of which has been attributed to the land-sea thermal contrast. Land surface characteristics of the continents have been suggested as an important factor in the modulation of the monsoon circulation and surface hydrology (Webster, 1987). A number of studies have explored the roles of land surface processes and the mechanisms that govern land-atmosphere interactions in the monsoon systems (e.g., Meehl, 1994; Zeng et al., 1998; Webster et al., 1998; Liu and Wu, 1997; Sun et al., 2001; Wu et al., 2002). For example, the relative roles of land surface evaporation and sea surface temperature (SST) on the Asian monsoon have been investigated using GCM simulations (Yang and Lau, 1998; Lau and Bua, 1998). They found that the land surface had substantial but limited effects at local scales. Using two different land surface schemes, one with and the other without explicit vegetation parameterization but keeping the same surface albedo, it was also found that two land surface schemes produced similar results at the planetary scale, but

*E-mail: liwp@cma.gov.cn

substantial differences at regional scales occurred, especially in the monsoon regions and some of the large continental areas (Xue et al., 2004).

With the increase of knowledge about vegetation biophysical process, changes in vegetation feedback into the climate have been widely investigated by GCM simulations for South America (e.g., Lean and Warrilow, 1989; Norbe et al., 1991; Hoffmann and Jackson, 2000), tropical Africa (e.g., Xue, 1997; Zeng and Neelin, 2000), and tropical Asia (Mabuchi et al., 2005). An idealized GCM simulation of the desertification in Mongolian and Inner Mongolian grassland (Xue, 1996) produced negative monsoon rainfall anomalies in northern and southern China and positive rainfall anomalies along the Yangtze River region, which were generally consistent with the observed decadal anomalies between the 1980s and the 1950s. The large reduction in evaporation due to land degradation resulted in less convection and lowered atmospheric heating rates, which were associated with relative subsidence and, in turn, weakened the northward movement of the monsoon flow and lowered the rainfall and evaporation, leading to a positive feedback system. In recent studies using regional circulation models, it was found that increase of vegetation cover lowered surface temperature, enhanced precipitation and surface runoff in north China (Lu and Chen, 1999; Zheng et al., 2002).

Observational studies have also indicated that a strong link exists between vegetation and climate. In their statistical studies, Zhang et al. (2003a,b) showed that correlations between spring NDVI and the following summer precipitation in the eastern arid/semi-arid region of China (including Inner Mongolia and part of the Yellow River basin) were significant, but the vegetation-temperature relationship was much weaker. Because many feedbacks are involved in the vegetation-climate interaction, the mechanism was not clearly understood through statistical analysis, which might be addressed by numerical experiments.

Defined as the ratio of leaf area to land surface area in a vertical column, the leaf area index (LAI) is a representation of the density of vegetation at the surface. It has been used in vegetation models to regulate the radiative transfer and the amount of transpiration from the surface and thereby controlling the partition of surface heat flux. Generally speaking, transpiration and interception loss increase with the increased leaf area in the column while the surface sensible heat flux decreases, which affects the atmospheric circulation and the associated precipitation (Chase et al., 1996). But the LAI index was usually prescribed according to seasonal cycle in the land surface schemes and therefore it had no interannual variation, which suppressed the influence of vegetation in modulating the climate interannual variability, even though the scheme with explicit vegetation parameterization performed well in simulating seasonal monsoon development (e.g., Xue et al., 2004), which was one of the motivations to conduct this numerical study.

The results of a recent numerical simulation of the impact of vegetation cover variability on North American monsoon (Matsui et al., 2005) indicated a negative vegetation-rainfall feedback rather than the supposed positive feedback, the least vegetation cover produced the most evaporation and rainfall. It was pointed out that the parameterization scheme in their land surface model and only one vegetation index (coverage) was investigated in their experiments might be responsible for this. Considering the dependence on large-scale background circulation when addressing the effect of land surface change (Dirmeyer and Shukla, 1996), we conducted this numerical simulation for East Asia, where the general circulation pattern is quite different from that in North America, using a Simplified Simple Biosphere land surface scheme (SSiB, Xue et al., 1991), a different scheme from what Matsui used in their study. Besides, different than using idealized land surface change in previous simulations, realistic vegetation indexes derived from satellite observation were employed in this study.

In this paper, we investigate the influence of both LAI and fractional vegetation cover (FVC) on East Asia summer monsoon using SSiB coupled to the National Center for Environmental Prediction (NCEP) GCM, focusing on the Yellow River basin (YRB), where vegetation coverage changed substantially from 1987 to 1988 and the associated climate variation is supposed to be significant. The data used and experiment design are given in the second section. Vegetation changes from 1987 to 1988 and variations of precipitation and surface temperature between these two years are discussed in the third section. The associated surface climate changes are presented in the fourth section. The possible mechanisms involved are investigated in the fifth section. A summary and discussions are given in the sixth section.

2. Data and experiment design

Two sets of numerical experiments were conducted by using NCEP GCM coupled with SSiB. The model has 18 vertical layers with a T42 horizontal resolution (slightly less than 3° in the mid-latitudes). One set employed a prescribed LAI (Dorman and Sellers, 1989) according to the vegetation distribution in SSiB (Xue

et al., 2001); the other used LAI and FVC from the International Satellite Land Surface Climate Project (ISLSCP, Los et al., 2000), which were derived based on satellite observations and are widely used in climate studies. We refer to these two sets of experiments as the control and test experiments, respectively, each of which consists of six cases. They start from 1st, 3rd, and 4th May of 1987 and 1988 and are integrated to the end of the year with observed SST. The initial atmospheric conditions and initial soil temperature are from the NCEP reanalysis data (Kalnay et al., 1996). The initial soil moisture is from the Global Soil Wetness Project (GSWP, Dirmeyer et al., 1999), a pilot study intended to produce a global dataset of soil wetness by using 1987 and 1988 meteorological observations and analyses to drive land surface models. It is expected that the soil moisture products from this project would be the best available data for GCM initial soil moisture conditions (Dirmeyer, 2000). SSiB participated in this project and the results produced by SSiB were used for this study. The averages for three initial conditions with different years for the control experiments are referred to as Case C87, Case C88, and those for test experiments as Case I87, and Case I88, respectively.

The June-July-August (JJA) mean differences between 1987 and 1988 are compared to investigate the influence of LAI and FVC on summer precipitation interannual variation in East Asia. The difference of Case C88–Case C87 is referred to as Case C and Case I88–Case I87 is referred to as Case I in this paper. In a qualitative sense, Case C indicated the influence of the interannual variation of SST, for the same set of vegetation indexes is used in Case C87 and Case C88, whereas Case I reveals the influence of both vegetation and SST. The comparison between Case C and Case I might give us some insights on the influence of vegetation on the interannual variation of summer rainfall. Precipitation data from the Climate Prediction Center Merged Analysis of Precipitation (CMAP, Xie and Arkin, 1997) and NCEP reanalysis data were employed to analyze these simulations.

3. Interannual variation of vegetation, precipitation and surface temperature

3.1 *Vegetation indexes*

Figure 1 shows the geographical distribution of FVC from ISLSCP in 1987 and the difference between 1987 and 1988. The eastern part of Northeast China, the upper reaches of the Yellow River, and the southeastern Tibetan Plateau are mostly covered by vegetation (more than 90%). Most parts of East China have an FVC value greater than 0.6. The difference of the vegetation cover between 1987 and 1988 exhibits a northeast-southwest orientated band from eastern Inner Mongolia to the YRB and eastern Tibetan Plateau, and a greater than 0.1 increase in FVC occurs in the eastern YRB (Fig. 1b), indicating that the interannual variation of vegetation in the semi-arid regions is remarkable.

The distribution of LAI is displayed in Fig. 2. Generally speaking, the LAI is greater than 4 in forest areas, such as in the eastern part of Northeast China and along the Qinling Mountains and Hanjiang River Basin to the south of the YRB. LAI varies between 2 and 4 in most parts of East China, whereas in arid/semi-arid areas like Inner Mongolia and the north part of the YRB, LAI is less than 2 or smaller. There is an unrealistic peak of vegetation coverage and high LAI around 34°N and 103°E, which is a transition area from the Hanjiang River Basin and the Qingling Mountains to the Qinghai-Tibetan Plateau. The topographic effect and cloud contamination may contribute to the problem. We refer this area as Area X in this paper. Similar to Fig. 1b, the major difference of JJA LAI between 1987 and 1988 is in eastern Inner Mongolia and the YRB, where the LAI value is relatively small. Vegeta-

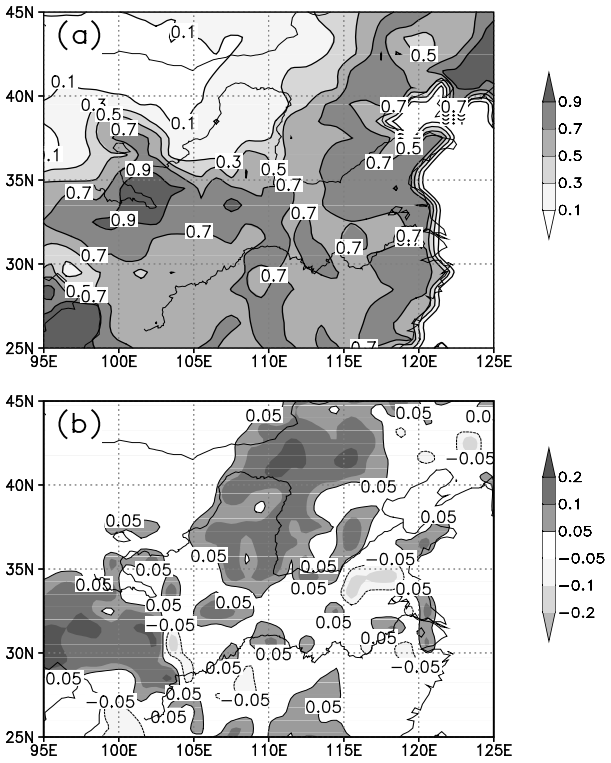

Fig. 1. Geographical distribution of yearly fractional vegetation cover from ISLSCP: (a) 1987, (b) the difference between 1988 and 1987. Only ±0.05 contours are displayed in (b) for the sake of clarity.

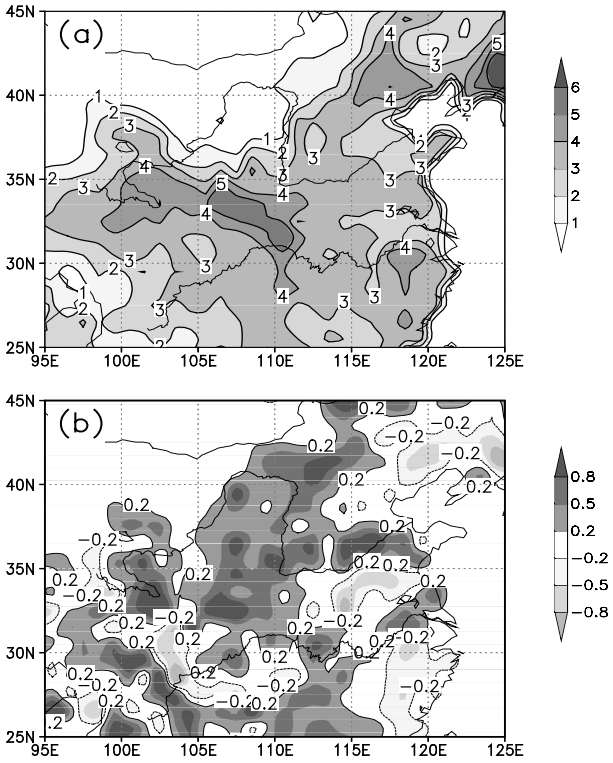

Fig. 2. Geographical distribution of JJA mean LAI from ISLSCP: (a) 1987, (b) the difference between 1988 and 1987. Only ±0.2 contours are displayed in (b).

tion is vulnerable in the transition area between the moist and dry land surfaces. Therefore, it is a sensitive indication of climate change, which may also in turn exert an influence upon the local climate. The following analyses are focused on the YRB, where the vegetation changes are relatively large and the differences of local summer climate conditions between 1987 and 1988 are statistically significant in the simulations.

3.2 *Precipitation and surface temperature*

JJA 1988 was wetter than JJA 1987 in the YRB and on its east flank (Fig. 3a), which coincided with the increased vegetation growth in 1988 (Figs. 1b, 2b). The region between the Yellow River and the Yangtze River was drier in 1988 (a La Niña year) than in 1987 (an El Niño year). In Case C, however, large parts of the YRB were drier in 1988 and the wetter region was restricted to a much smaller area of the lower reaches of the Yellow River (Fig. 3b). The simulations in Case I, which includ both the SST and vegetation effect, were better than Case C with the proper wet area in the YRB. But the wet center shifted southeastward compared to the observation. The model produced more precipitation over the area with more vegetation (Figs. 1b, 2b, and 3c). The unrealistic vegetation in Area X (Figs. 1b and 2b) is likely to have produced a

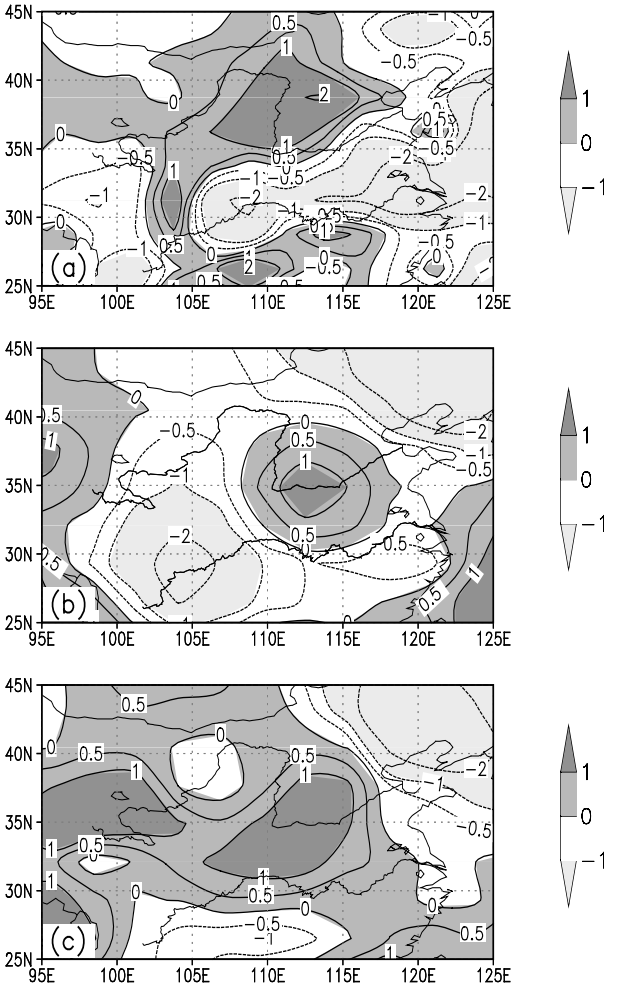

Fig. 3. Difference of JJA mean precipitation (mm d^{-1}) between 1988 and 1987. Contour interval is 0.5 mm d^{-1}. (a) Observation, (b) Case C, and (c) Case I.

wet area to the southwest of the YRB. Both Case C and Case I produced a larger than observed dry bias in northeastern China. Neither simulation captured the dry area between the Yellow River and the Yangtze River. This reveals the complexity and challenge in simulating East Asian monsoon precipitation.

Redistribution in surface water and energy balances due to changes in the surface vegetation conditions led to surface temperature changes from 1987 to 1988. In the NCEP reanalysis, there was a cold center in the YRB and on its east flank, surrounded by warm areas, which is generally consistent with the precipitation distribution in Fig. 3a. The cold center was shifted southeastward and restricted to the lower reaches of the Yellow River in Case C (Fig. 4b) but was fairly well reproduced in the YRB in Case I, partly attributable to more vegetation transpiration in Case I.

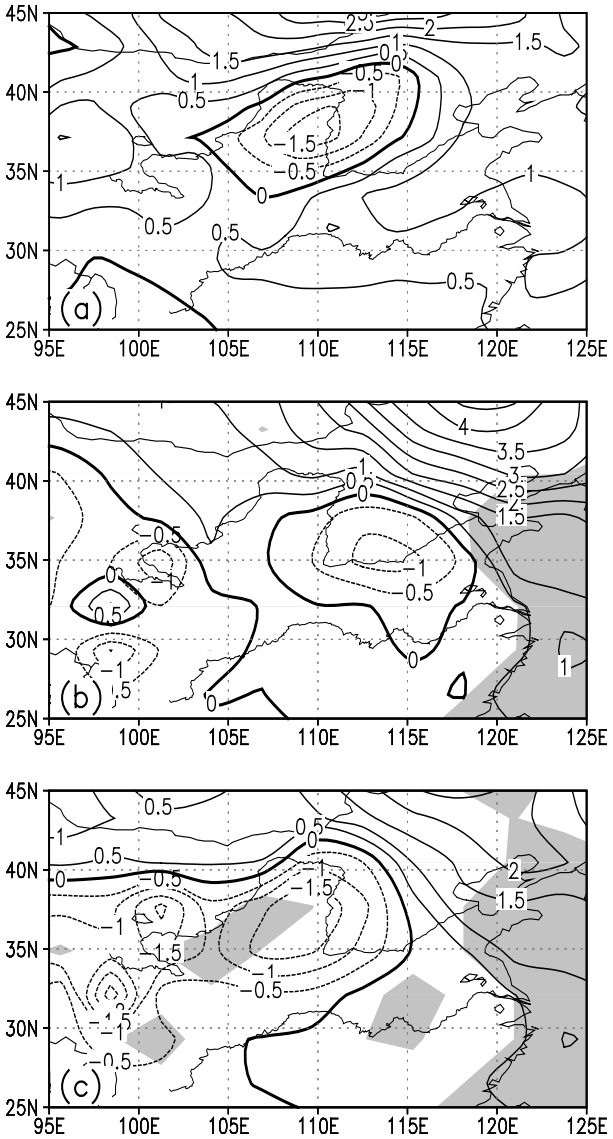

Fig. 4. Difference of JJA mean surface temperature (°C) between 1988 and 1987. Contour interval is 0.5°C. (a) NCEP reanalysis, (b) Case C, (c) Case I. Shading indicates significance at the 95% level of the student's t-test.

But a cold center appeared around the upper reaches of the Yellow River (Fig. 4c), which was again relevant to the anonymous vegetation changes in the ISLSCP data as pointed out earlier. Comparing Figs. 3c and 4c with Figs. 1b and 2b, it seems that changes in vegetation are more closely related to temperature than precipitation. Further analysis shows that greater vegetation growth lowered the maximum surface temperature and therefore reduced the diurnal temperature variation in Case I, which was much closer to that in the NCEP reanalysis than in Case C (not shown).

To investigate the reason that causing the aforementioned precipitation and surface temperature variations, we analyzed the low cloud coverage which plays an important role in radiative transfer and convective rainfall formation. The two sets of experiments produced quite different characteristics in low cloud coverage. Case C exhibited more cloud to the east of the YRB and the area between the lower reaches of the Yellow River and the Yangtze River (Fig. 5b), corresponding to the greater rainfall center (Fig. 3b) and cooler surface (Fig. 4b), while the less cloud in the southwestern YRB is very consistent with the drought there. Closer to the NCEP reanalysis, Case I produced more cloud over almost all of the YRB and to its east, corresponding to the better vegetation growth there and in the downstream region (Fig. 5c). This is in line with the statistical analysis of the vegetation condition and precipitation of Zhang et al. (2003b), which investigated the relationship between spring NDVI and the following summer rainfall.

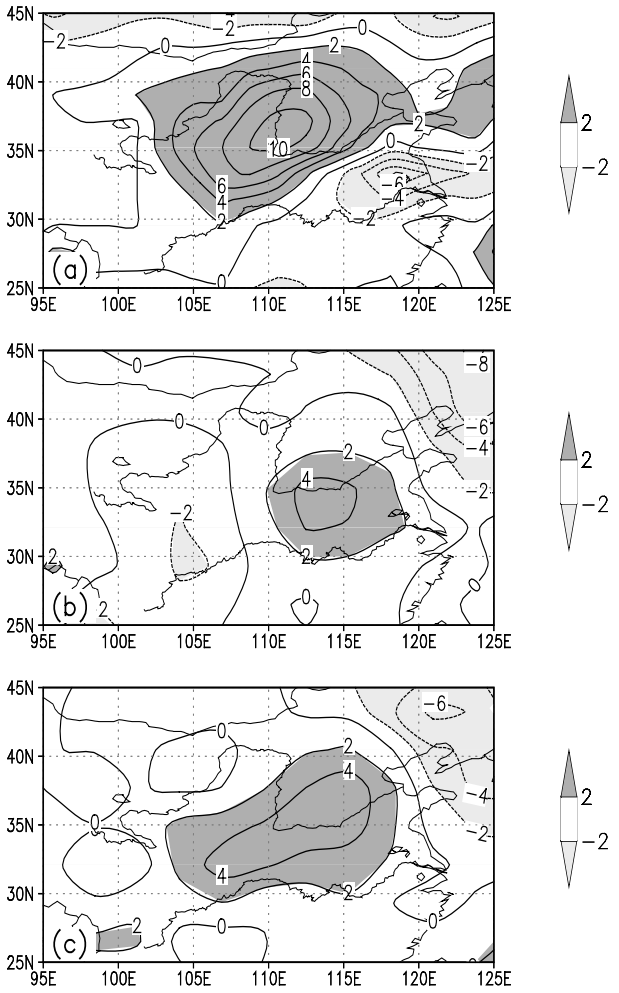

Fig. 5. JJA mean low cloud coverage difference between 1988 and 1987: (a) NCEP reanalysis, (b) Case C, (c) Case I.

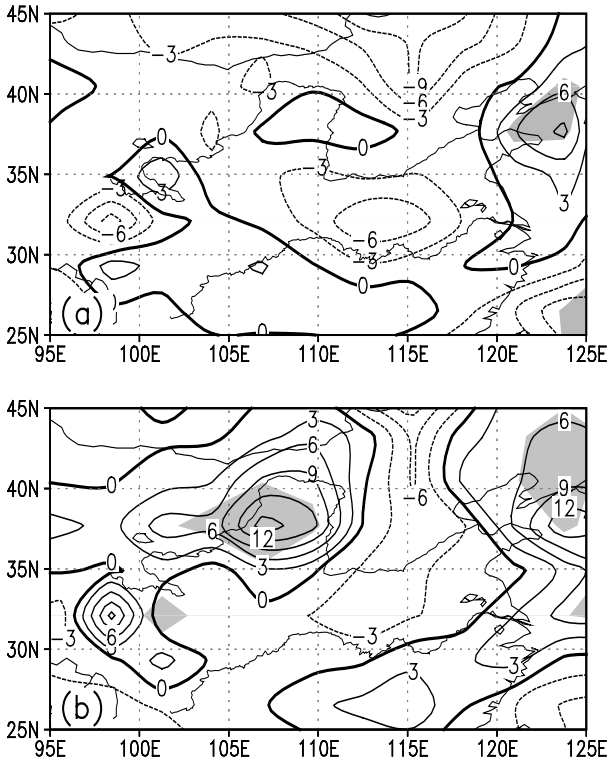

Fig. 6. Difference of JJA mean net surface radiation (W m^{-2}) between 1988 and 1987. (a) Case C, (b) Case I. Shading indicates significance at the 95% level of the student's t-test.

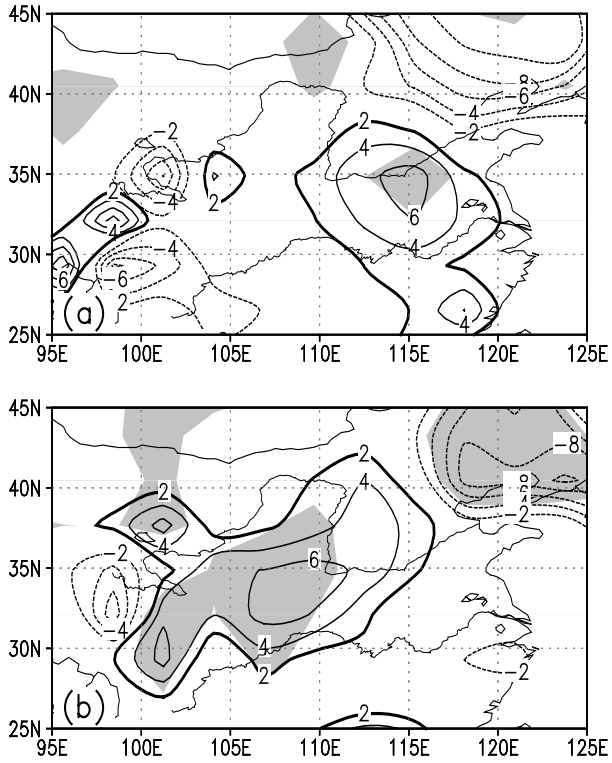

Fig. 7. Difference of JJA mean canopy interception loss (W m^{-2}) between 1988 and 1987. (a) Case C, (b) Case I. Shading indicates significance at the 90% level of the student's t-test.

From the above analyses, Case I, which includes both SST and vegetation effects, performed better in the simulations of interannual climate variation than Case C, which used prescribed FVC and LAI index with no interannual variation, especially in the YRB where vegetation experienced considerable variation from 1987 to 1988, indicating the potential of using realistic vegetation indexes in land surface schemes to improve climate prediction.

4. Surface climate variations in response to vegetation changes

Surface albedo (not shown) decreased slightly in the YRB in Case I, corresponding to the higher vegetation growth in 1988, whereas surface albedo almost remained unchanged in Case C because vegetation was the same in Case C87 and Case C88. Undoubtedly, changes in surface albedo, surface temperature and cloud coverage lead to net surface radiation variations. In Case C, net surface radiation decreased slightly in most parts of the YRB (Fig. 6a). The effects of net solar radiation and net longwave radiation almost balanced each other in the YRB (not shown), but in the area between the lower reaches of the Yellow River and the Yangtze River, less solar radiation due to increased low cloud coverage dominated, resulting in the decrease of net radiation there. In Case I, the net surface solar radiation increased slightly in the northwest part but decreased in the other parts of the YRB and the surrounding areas, whereas net surface longwave radiation loss decreased in the whole YRB because of the decrease of upward longwave radiation (not shown) due to lower surface temperature (Fig. 4c). Net surface radiation increased in a statistically significant way by more than 10 W m^{-2} in the YRB (Fig. 6b) where vegetation coverage and density increased in 1988 (Figs. 1b, 2b).

Canopy interception of precipitation depends on vegetation properties as well as the amount of rainfall. In the semi-arid YRB area, precipitation may dominate the magnitude of interception. The canopy interception change in Case C was mainly a response to the changes in precipitation, for the same set of vegetation indexes were employed for 1987 and 1988 (Figs. 7a, 3b). Corresponding to the interannual variation of LAI and FVC, Case I produced more interception than Case C along the northeast-southwest vegetation increase band around YRB where summer precipitation increased as well (Figs. 7b, 1b and 3c). But interception decreased in most parts of Northeast China

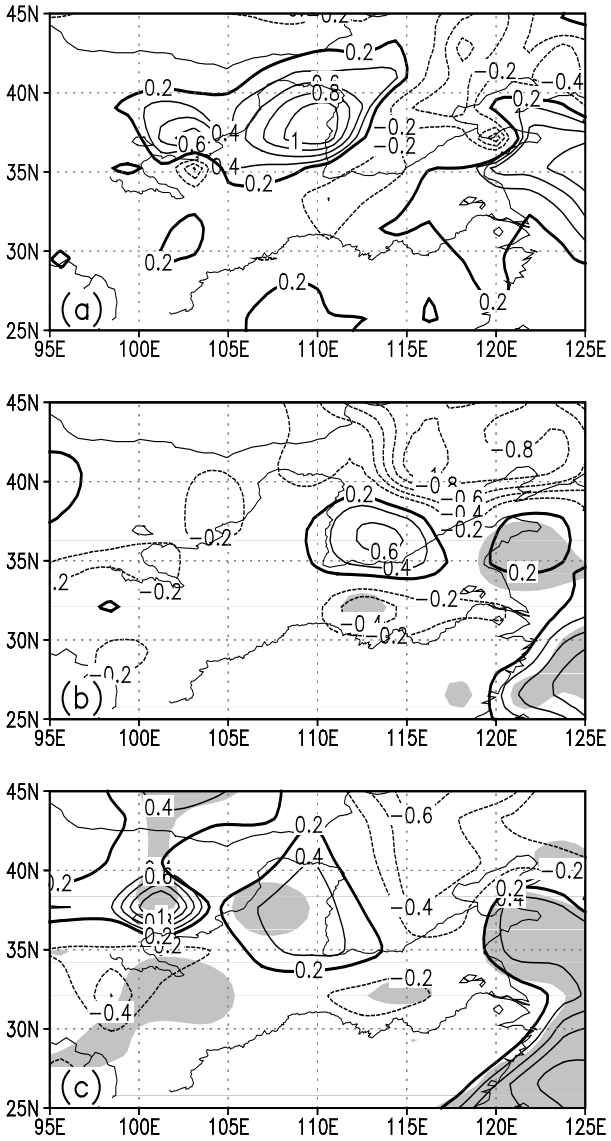

Fig. 8. Difference of JJA mean surface evaporation (mm d^{-1}) between 1988 and 1987. (a) NCEP reanalysis, (b) Case C, (c) Case I. Shading indicates significance at the 95% level.

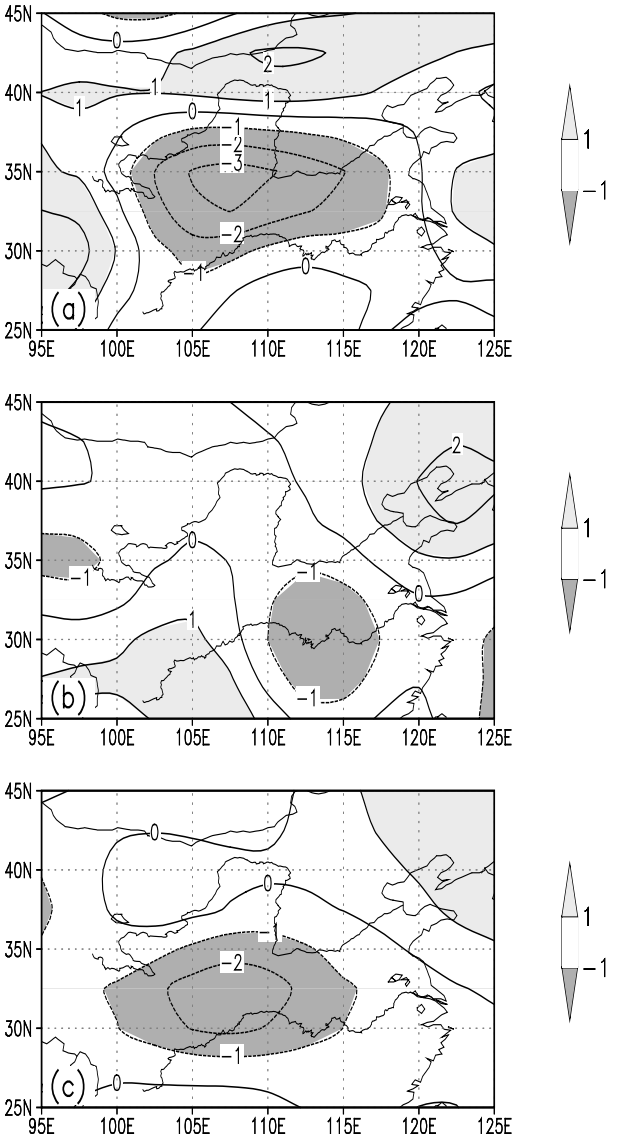

Fig. 9. Difference of JJA mean pressure velocity (0.01 Pa s^{-1}) at 850 hPa between 1988 and 1987. (a) NCEP reanalysis, (b) Case C, (c) Case I.

where precipitation decreased in both Case C and Case I, although vegetation changed very slightly there.

As a direct response to precipitation, top layer soil wetness increased in the YRB in Case I and along the lower reaches of the Yellow River in Case C (not shown), corresponding to the increases of precipitation shown in Fig. 3. Consequently, the surface temperature lowered (Fig. 4) and sensible heat flux decreased in the above areas (not shown).

The contrast in surface latent heat flux (represented by evaporation, Fig. 8) between Case I and Case C is also pronounced. In Case I, the YRB experienced more evaporation in 1988 than in 1987, which is much closer to the NCEP reanalysis than Case C. The localized evaporation increase to the west of the YRB in Case I corresponded to the area around Qinghai Lake. In Case C, the high evaporation area was located in the lower reach of the Yellow River, shifting eastward from the location in the NCEP reanalysis. The evaporation decreased in the western YRB, in contrast to that in the NCEP reanalysis and Case I. Please note that, due to the surface parameterizations in the reanalysis model, the surface variables in the reanalysis data are not reliable (e.g., Xue et al., 2001). The comparisons in this paper emphasize the general patterns rather than the absolute values.

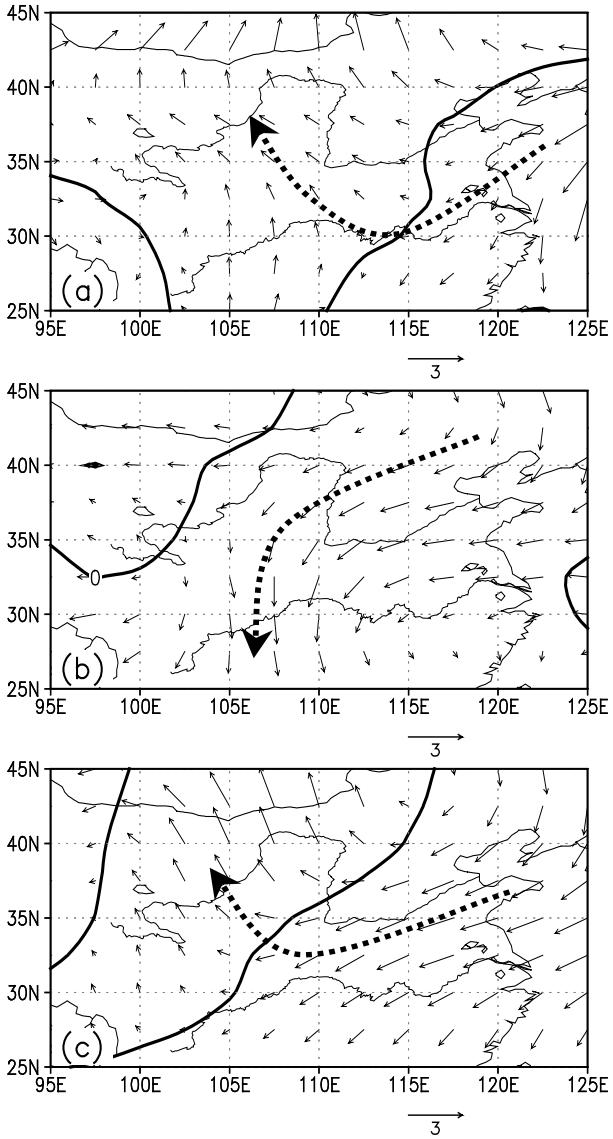

Fig. 10. Difference of JJA mean 850-hPa wind vector (m s^{-1}) between 1988 and 1987. (a) NCEP reanalysis, (b) Case C, (c) Case I. To clarify the circulation patterns, the bold lines show the locations where the meridional wind is zero, and the dotted arrow in each panel highlights the dominant flow pattern.

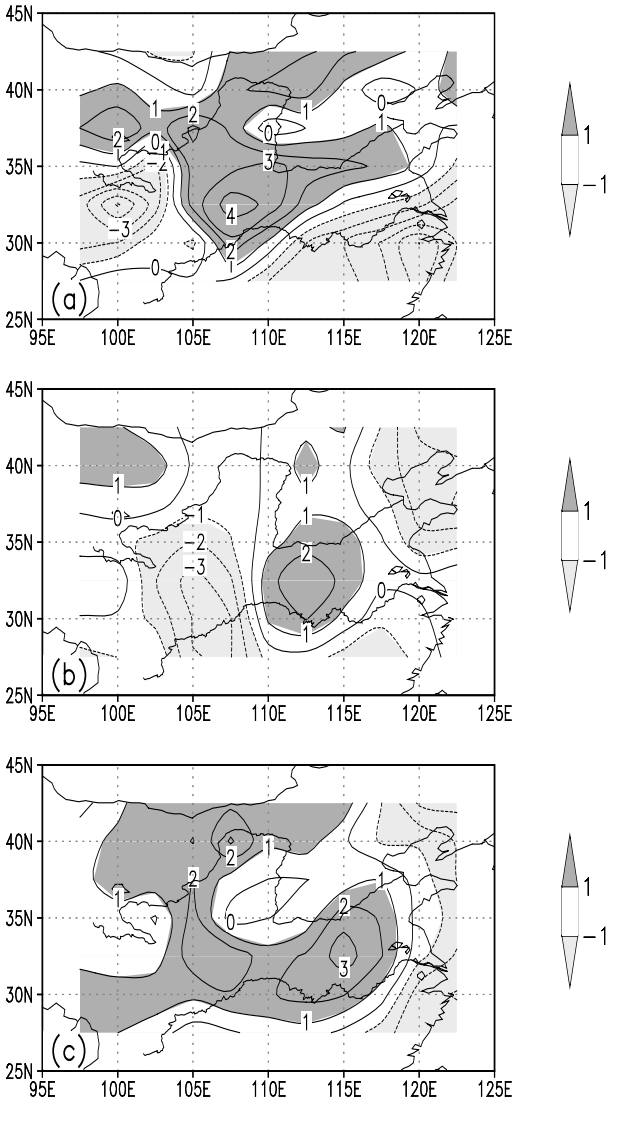

Fig. 11. Difference of JJA mean column-integrated moisture flux convergence (mm d^{-1}) between 1988 and 1987. (a) NCEP reanalysis, (b) Case C, (c) Case I.

5. Variations in circulation and moisture flux

Land surface processes exert an influence upon the atmospheric circulation by heating or cooling the overlying air. Changes in precipitation are closely linked to the atmospheric circulation and the associated moisture flux.

The vertical pressure velocity at 850 hPa in Case I agreed well with the NCEP reanalysis, with a relatively strong upward motion center overlying the southern part of the YRB and much weaker downward motion to the north, whereas in Case C, upward motion spanned from the northern YRB southeastward to the lower reaches of the Yangtze River and downward motion to the south (Fig. 9). The upward motion centers are located a little bit southward to where the low cloud coverage increased in Fig. 5.

In addition to the above mentioned vertical movement, Case C and Case I also showed quite different horizontal circulation patterns. At 850 hPa, for example, clockwise circulation prevailed to the north of 32°N in Case I, which was similar to that in the NCEP reanalysis, except that the southerly-control area was

shrunk westward and less extensive in Case I. In contrast, Case C displayed a strong counter-clockwise circulation affecting almost the entire studied region (Fig. 10). The southeasterly wind over the YRB in the NCEP reanalysis and Case I favored more water vapor transport to the YRB from the ocean on the east or the relatively wet surface in the south, whereas the prevalent northeasterly in Case C hindered moisture converging to the YRB, which can be clearly shown in the moisture flux as follows.

Figure 11 displays the vertically integrated moisture flux and its convergence. The moisture convergence around the YRB in Case I and the reanalysis is consistent with the precipitation increases in their results. In Case C, the moisture convergence is located between the lower reaches of the Yellow River and the Yangtze, which corresponded to the precipitation increase. The moisture divergence in the western YRB and to its south is consistent with the precipitation decrease there (Fig. 11b and Fig. 3b). Comparisons of Figs. 3, 8, and 11 imply that both local evaporation and moisture convergence contributed to the interannual variation of precipitation around the YRB. Local evaporation plays an important role in central and northern YRB, whereas moisture flux convergence seemed to be more dominant in the southern YRB and to its south.

The aforementioned analyses are the JJA mean conditions. Table 1 displays the regional monthly mean precipitation averaged over the YRB during boreal summer. Case I produced a better simulations than Case C in most of the months in both 1987 and 1988 except for August in 1987. The differences between 1987 and 1988 in Case I are also closer to observation than Case C from June to August. In this study, less rainfall occurred in June 1988 than June 1987 in this area, although the JJA mean of 1988 had more rainfall, indicating the complexity of the interannual variation of precipitation in the YRB, which adds difficulties to the prediction of East Asia summer monsoon precipitation.

Table 1. Regional monthly mean of precipitation averaged for the Yellow River basin (35–42°N, 105–115°E).

Year	Month	CMAP	Case I	Case C
1987	June	2.38	2.32	1.56
	July	1.71	2.39	2.66
	August	3.11	3.57	3.43
1988	June	1.83	1.86	1.73
	July	4.29	3.59	3.52
	August	3.84	4.19	2.47
Difference	June	−0. 55	−0.46	0.17
1988–87	July	2.59	1.20	0.85
	August	0.73	0.61	−0.96

6. Summary and discussions

From the analyses of this study, changes in vegetation (fractional coverage, leaf area index) and the consequent changes in surface albedo and surface net radiation lead to variation in the surface energy partition in sensible and latent heat fluxes, influencing atmospheric circulation and the associated moisture flux, resulting in interannual variations of precipitation, canopy interception and soil moisture. Although vegetation growth responding to climate change is not addressed in this study, the changed physical conditions undoubtedly have an impact upon vegetation growth, closing the vegetation-climate feedback loop, which can be illustrated in Fig. 12. The small words superimposed on the arrows highlight the possible physical processes involved to establish the feedbacks, solid arrows indicate positive contributions whereas dotted arrows negative contributions. Where more than one process is involved, a thinner arrow represents a relatively less contribution in the feedback, say albedo is outweighed by cloud coverage in the surface solar radiation budget and surface longwave radiation outdid solar radiation in the net surface radiation balance. It should be pointed out that the above results are based on numerical simulations for 1987 and 1988 in the YRB area using SSiB coupled to NCEP/GCM, more cases by using different models for other geographic locations are necessary for drawing general conclusions.

Our statistical analysis showed that monthly LAI and precipitation averaged over the YRB for the period of 1982 to 1990 have the best correlation (0.291) when precipitation leads LAI by one month, higher than the zero-lag correlation coefficient of 0.286, both of which are significant at the 99% confidence level, indicating that the vegetation grows better (or worse) in response to more (less) precipitation in this semiarid area where precipitation plays a dominant role in vegetation growth. But the correlation when precipitation lags LAI by one month is much weaker (0.086), implying the complex relationship between vegetation and local climate and different time scales are involved in establishing the feedback. It must be pointed out that the simulation of the East Asian monsoon and the associated precipitation is very difficult due to the complex mechanisms involved in East Asia, e.g., the land-sea contrast, the complex topography and the influence of the Tibetan Plateau. The main purpose of this work is to show how the atmosphere responds to vegetation indexes such as the FVC and LAI.

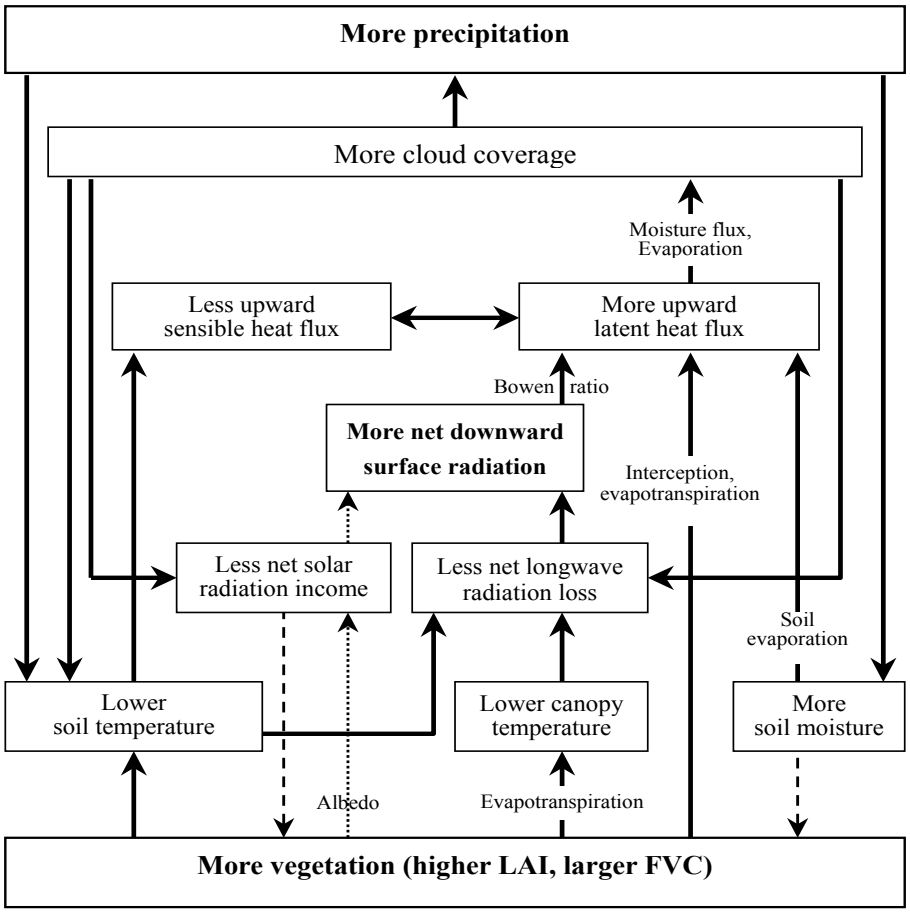

Fig. 12. A schematic diagram displaying the relationship between vegetation and precipitation. The small words superimposed on the arrows between two boxes indicate possible processes that establish the feedbacks. A thin dotted arrow indicate negative contribution but is outweighed by positive contribution represented by a thick solid arrow where more than one process is involved. The dashed arrows imply links not included in this study.

The relative importance of FVC and LAI to the climate could not be discriminated in our current experiment, for both factors were included in the experiment. We focused on the impact of vegetation on local climate around the Yellow River basin. Remote influences were not addressed in this study. Besides, the recycling rate of precipitation, local evaporation versus moisture flux along with the above points deserve further investigation.

In this numerical experiment study, the interannual variations of vegetation indexes (FVC and LAI) were prescribed according to the satellite observations. Vegetation had no response to the changed climate. The land-atmosphere interaction is a one-way forcing in this case. Undoubtedly, a dynamic parameterization scheme that can simulate the biophysical growth of vegetation is desirable to investigate the realistic vegetation-atmosphere interaction, which is our future study topic. In addition, a nested regional model within a GCM would be desirable to more realistically study the regional climate in detail.

In previous idealized numerical simulations about the impact of vegetation on climate, land surface usually underwent dramatic changes, which might enlarge the response of climate. Our study using somewhat "realistic" vegetation index derived from satellite observations produced better results than that without interannual variation of vegetation, indicating the potential of using realistic vegetation condition in climate prediction.

Concerning the ecosystem vulnerability in arid/semi-arid areas, deforestation and degradation induced by human activities will exacerbate drought in a positive feedback system, and this will contribute to sand storms by feeding more sand from the degraded land surface. Measures should be taken to protect the dete-

riorating ecosystem in arid/semi-arid regions like the Yellow River Basin.

Acknowledgments. This work was jointly supported by the Ministry of Science and Technology of China through public welfare funding under Grant No. 2002DIB20070, by China Meteorological Administration grant CCSF 2005-1, and by the National Natural Science Foundation Grant NSF-ATM-0353606. The model runs were carried out on the NCAR supercomputers. Comments and suggestions from Prof. Wu Guoxiong and Prof. Ji Jinjun of IAP/LASG and two anonymous reviewers to greatly improve the manuscript are really appreciated.

REFERENCES

Chen Longxun, Zhu Qiangen, and Luo Huibang, 1991: *East Asian Monsoon*. China Meteorology Press, Beijing, 362pp. (in Chinese)

Chase, T. N., R. A. Pielke, T. G. Kittel, R. Nemani, and S. W. Running, 1996: Sensitivity of a general circulation model to global changes in leaf area index. *J. Geophys. Res.*, **101**(D3), 7393–7408.

Dirmeyer, P. A., 2000: Using a global soil wetness dataset to improve seasonal climate simulation. *J. Climate*, **13**, 2900–2922.

Dirmeyer, P. A., and J. Shukla, 1996: The effect on regional and global climate expansion of the world's deserts. *Quart. J. Roy. Meteor. Soc.*, **122**, 451–482.

Dirmeyer, P. A., A. J. Dolman, and Nobuo Sato, 1999: The pilot phase of the Global Soil Wetness Project. *Bull. Amer. Meteor. Soc.*, **80**, 851–878.

Dorman, J. L., and P. J. Sellers, 1989: A global climatology of albedo, roughness length and stomatal resistance for atmospheric general circulation models as represented by the Simple Biosphere Model (SiB). *J. Appl. Meteor.*, **28**, 833–855.

Hoffmann, W. A., and R. B. Jackson, 2000: Vegetation-climate feedbacks in the conversion of tropical savanna to grassland. *J. Climate*, **13**, 1593–1602.

Kalnay, E., and Coauthors, 1996: The NCEP/NCAR 40-year reanalysis project. *Bull. Amer. Meteor. Soc.*, **77**, 437–471.

Lau, K.-M., and W. Bua, 1998: Mechanisms of monsoon-Southern Oscillation coupling: Insights from GCM experiments. *Climate Dyn.*, **14**, 759–779.

Lean, J., and D. A. Warrilow, 1989: Simulation of the regional climatic impact of Amazon deforestation. *Nature*, **342**, 411–413.

Liu Hui, and Wu Guoxiong, 1997: Impacts of land surface on climate of July and onset of summer monsoon–A study with an AGCM plus SSiB. *Adv. Atmos. Sci.*, **14**, 289–308.

Los, S. O., and Coauthors, 2000: A global 9-year biophysical land surface data set from NOAA AVHRR data. *J. Hydrometeolorogy*, **1**, 183–199.

Lu Shihua, and Chen Yuchun, 1999: The influence of northwest China afforestation on regional climate in China. *Plateau Meteorology*, **18**, 416–424. (in Chinese)

Mabuchi, K., Y. Sato, and H. Kida, 2005: Climatic Impact of Vegetation Change in the Asian Tropical Region. Part I: Case of the Northern Hemisphere Summer. *J. Climate*, **18**, 410–428.

Matsui, T., V. Lakshmi, and E. E. Small, 2005: The effects of satellite-derived vegetation cover variability on simulated land-atmosphere interactions in the NAMS. *J. Climate*, **18**, 21–40.

Meehl, G. A., 1994: Influence of the land surface in the Asian summer monsoon: External versus internal feedbacks. *J. Climate*, **7**, 1033–1049.

Norbe, C. A., P. J. Sellers, and J. Shukla, 1991: Amazonian deforestation and regional climate change. *J. Climate*, **4**, 957–988.

Sun Lan, Wu Guoxiong, and Sun Shufen, 2001: Numerical simulations of land surface processes on climate-implementating of SSiB in IAP/LASG AGCM and its performance. *Acta Meteorologica Sinica*, **15**(2), 160–177.

Webster, P. J., 1987: The elementary monsoon. *Monsoons*, J. F. Fein and P. L. Stephens, Eds., John Wiely, New York, 3–32.

Webster, P. J., V. Magana, T. N. Palmer, J. Shukla, R. A. Tomas, M. Yanai, and T. Yasunari, 1998: Monsoons: Processes, predictability, and the prospects for prediction. *J. Geophys. Res.*, **103**(C7), 14451–14510.

Wu Guoxiong, Sun Lan, Liu Yimin, Liu Hui, Sun Shufen, and Li Weiping, 2002: Impacts of land surface processes on summer climate. *Selected Papers of the Fourth Conference on East Asia and Western Pacific Meteorology and Climate*, C.-P. Chang et al., Eds., World Scientific, Singapore, 64–76.

Xie, P., and P. A. Arkin, 1997: Global precipitation: A 17-year monthly analysis based on gauge observations, satellite estimates and numerical model outputs. *Bull. Amer. Meteor. Soc.*, **78**, 2539–2558.

Xue, Y., 1996: The impact of desertification in the Mongolian and the Inner Mongolian Grassland on the regional climate. *J. Climate*, **9**, 2173–2189.

Xue, Y., 1997: Biosphere feedback on regional climate in tropical North Africa. *Quart. J. Roy. Meteor. Soc.*, **123B**, 1483–1515.

Xue, Y., P. J. Sellers, J. L. Kinter III, and J. Shukla, 1991: A simplified biosphere model for global climate studies. *J. Climate*, **4**, 345–365.

Xue, Y., F. J. Zeng, K. Mitchell, Z. Janjic, and E. Rogers, 2001: The impact of land surface processes on the simulation of the U.S. hydrological cycle: A case study of 1993 flood using the Eta/SSiB regional model. *Mon. Wea. Rev.*, **129**, 2833–2860.

Xue, Y., H.-M. H. Juang, W.-P. Li, S. Prince, R. DeFries, Y. Jiao, and R. Vasic, 2004: Role of land surface processes in monsoon development: East Asia and West Africa. *J. Geophys. Res.*, **109**, D03105, doi: 10.1029/2003JD003556.

Yang, S., and K.-M. Lau, 1998: Influences of sea surface temperature and ground wetness on Asian summer monsoon. *J. Climate*, **11**, 3230–3246.

Zhang Jingyong, Dong Wenjie, Ye Duzheng, and Fu Congbin, 2003a: New evidence for effects of land cover in China on summer climate. *Chinese Science Bulletin*, **48**, 401–405.

Zhang Jingyong, Dong Wenjie, Fu Congbin, and Wu Lingyun, 2003b: The influence of vegetation cover on summer precipitation in China: A statistical analysis of NDVI and climate data. *Adv. Atmos. Sci.*, **20**, 1002–1006.

Zeng Ning, and J. D. Neelin, 2000: The role of vegetation-climate interaction and interannual variability in shaping the African savanna. *J. Climate*, **13**, 2665–2670.

Zeng Qingcun, Dai Yongjiu, and Xue Feng, 1998: Simulation of the Asian Monsoon by IAP AGCM Coupled with an Advanced Land Surface Model (IAP94). *Adv. Atmos. Sci.*, **15**, 1–16.

Zheng Yiqun, Qian Yongfu, Miao Manqian, Yu Ge, Kong Yushou, and Zhang Donghua, 2002: The effects of vegetation change on regional climate I: Simulation results. *Acta Meteorologica Sinica*, **60**, 1–16. (in Chinese)